5478 *Macromolecules* **2009**, *42*, 5478–5485
DOI: 10.1021/ma9008737

Macromolecules
ARTICLE

Blue Emitting Polyfluorenes Containing Dendronized Carbazole and Oxadiazole Pendants: Synthesis, Optical Properties, and Electroluminescent Properties

Qiang Peng,*,† Jun Xu,† Mingjun Li,† and Wenxu Zheng‡

†*School of Environmental and Chemical Engineering, Nanchang Hangkong University, Nanchang 330063, P. R. China, and* ‡*Department of Applied Chemistry, College of Science, South China Agricultural University, Guangzhou 510642, P. R. China*

Received April 21, 2009; Revised Manuscript Received June 9, 2009

ABSTRACT: A series of new polyfluorenes with dendritic functional cabazole and oxazole side chains have been successfully designed, synthesized, and characterized. These copolymers show good thermal properties and solubility in organic solvents, such as THF, CH_2Cl_2, $CHCl_3$, toluene, etc. The photoluminescent (PL) and electroluminescent (EL) emission color quality was improved very much due to less aggregates of main chains of polyfluorenes (PFs) with the steric hindrance of dendritic functional carbazole and oxazole units. The electroluminescent devices based on these copolymers as blue emitters and host materilas were fabricated and evaluated. Balanced carriers and high efficiencies were obtained in both nonphosphorescent and phosphorescent PLEDs. The best devices were obtained by using PFCO1 materilas with the exteral quantum efficiencies of 1.03% for ITO/PEDOT/PFCO1/TPBI/LiF/Al and 11.63% for ITO/PEDOT/PFCO1:$(tpbi)_2$-Ir(acac)/Ca/Al. The results indicated that these copolymers were promising candicates for both efficient pure blue emitters and host materials for highly efficient phosphorescent PLEDs.

Introduction

Conjugated polymers have been extensively studied for their potential applications in large area full-color displays because of their easy processability, low driving voltage, wide viewing angle, and facile color tunability over the full range.[1] Recently, stable blue light emitting polymers with high efficiency have received considerable interest. Despite much effort on this topic, only a limited number of polymers exhibit promising performance for light emitting diodes.[2] Among them, polyfluorenes (PFs) have been emerged as promising blue light emitting materials because of their excellent thermal and chemical stability as well as high photoluminescence (PL) quantum efficiencies.[3] However, a major problem with PFs concerns their tendency to form long-wavelength aggregates/excimers or keto defects in the solid state upon thermal annealing or device operation, which leads to issues of color instability of the light emitted from the fabricated PLEDs.[4] The keto defects can be avoided by purification of monomers to a high degree prior to their polymerization.[4b,5] Various strategies have also been developed to reduce the formation of aggregation in PFs, which include the introduction of sterically hindered side chains or dendronization, incorporation of spiro-linked or cross-linked structures, and blending with a high glass transition temperature polymer to limit the chain mobility.[6]

Dendronized polymers have been proved to be a efficient way to suppress the formation of aggregates/excimers of PFs main chains because of the shielding effect provided by the dendritic side chains on the conjugated backbones. Research work regarding PFs modified with polyphenylene dendrons[7] or Fréchet-type dendrons[8] have been reported. Recently, some dendronized PFs containing functional carbazole or oxadiazole dendrons have been designed and attracted considerable attention, with their focal benzyl groups directly bonded to the C-9 carbon of the fluorene cycles.[8] These conjugated polymers have specific optical and physical properties as well as electronic properties with enhanced stability.[9]

Organic phosphorescent LEDs based on transition-metal complexes, such as Pt(II), Os(II), and Ir(III), have attracted great attention because of their potential for attaining high overall devices efficiency.[10] Polymer materials are expected to be promising host candicates for the phosphorescent devices due to their good thermal properties, excellent processability, and low price. Because the excitation of most phosphorescent emitters is in the blue region (400−450 nm), polyfluorene (PF) and poly(9-vinylcarbazole) (PVK) were usually used as host materials doped with phosphorescent complexes by a simple solution process.[11] Selecting host materials is crucial in enhancing the device efficiency during both Förster and Dexter energy transfer. In general, host materials should be selected to ensure that they have a higher triplet energy level than that of the phosphorescent emitters to enhance the energy transfer from the host to the guest while prohibiting the energy transfer of triplet excitons from the guest to the host material.[12] So there should be large overlap between the emission peaks of the host materials and the excitation spectra of the phosphorescent emitters, where the energy of the host materials after excitation can be transferred to the guest materials.[13] In addition, the charge transporting properties of host materials are also important. Combination of both hole-transport and electron-transport units can balance carriers for the phosphorescent LEDs. Phase separation and aggregation of phosphorescent emitters in polymer should also be taken into account.[14]

Therefore, we have embarked on the design, synthesis, and characterization of dendronized PFs with functional carbazole dendrons as well as oxadiazole dendrons together. Carbazole units are well-known hole-transporting groups as a result of the electron donating capabilities associated with its nitrogen atom.[15] Carbazole-based polymers, such as poly(vinylcarbazole) (PVK), are also used extensively as wide bandgap hosts to lower bandgap fluorophores. On the other hand, molecular and

*To whom correspondence should be addressed: e-mail qiangpengjohnny@yahoo.com.

 Published on Web 06/23/2009

Scheme 1. Synthesis Routes for the Monomers and Dendronized Copolymers

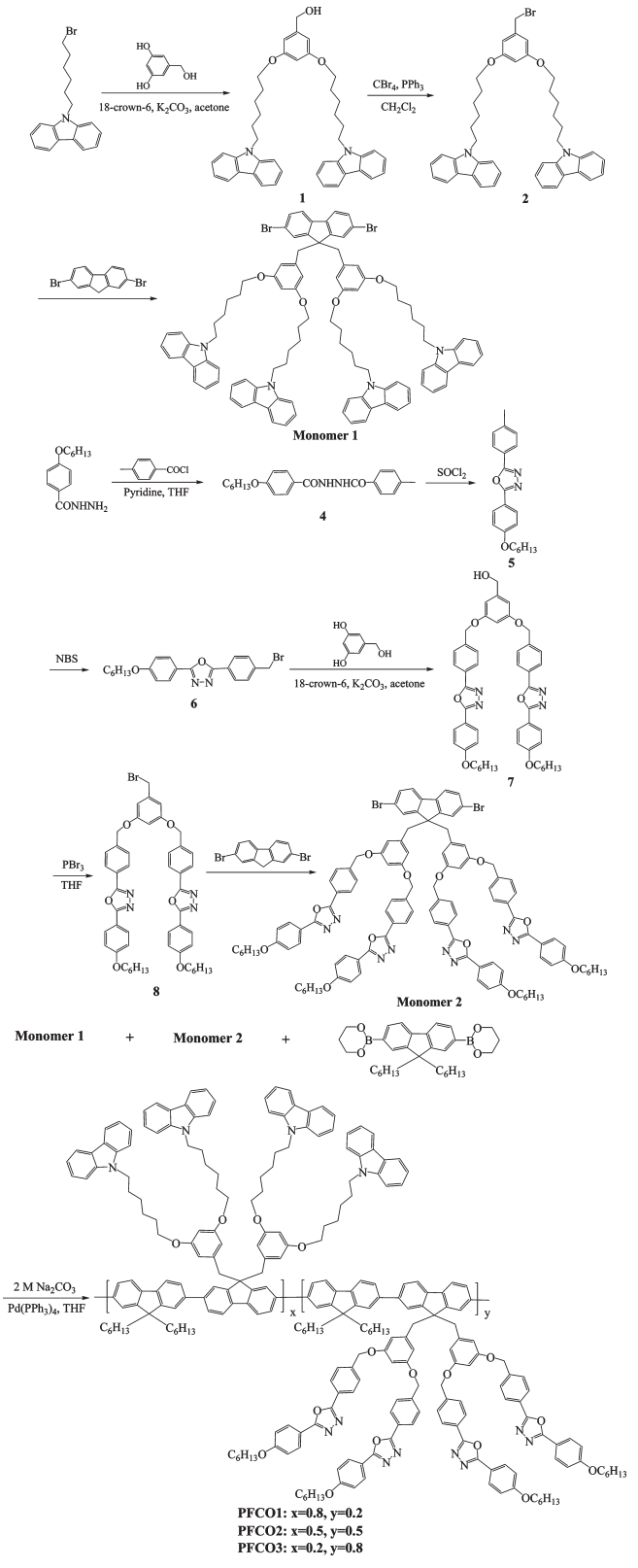

polymeric 1,3,4-oxadiazole (OXD) derivatives are the most widely studied classes of electron injection and/or hole-blocking materials, mainly because of their electron deficiency, high photoluminescence quantum yield, and good thermal and chemical stabilities.[16] To our knowledge, this work will be the first report of fluorene-based conjugated polymers incorporated with both carbazole and oxadiazole dendrons in the main chains for polymer light emitting diodes. The resulting polymers are expected to be used as high-performance light emitting materials with improved efficiency and blue color purity. Futhermore, these copolymer materials are anticipated to be used as host for phosphorescent LEDs with balanced carriers and efficient energy transfer.

Table 1. Molecular Weights and Thermal Properties of the Copolymers

copolymers	yield (%)	M_w[a] ($\times 10^3$)	PDI[a] (M_w/M_n)	T_d[b] (°C)	T_g[c] (°C)
PFCO1	82	19.6	1.82	393	101
PFCO2	80	20.2	1.96	401	98
PFCO3	77	34.1	2.03	409	86

[a]Molecular weights and polydispersity indices were determined by GPC in THF using polystyrene as standards. [b]Onset decomposition temperature measured by TGA under N_2. [c]Glass transition temperature measured by DSC under N_2.

Results and Discussion

Synthesis and Characterization. The synthetic routes of the monomers and the corresponding polymers are shown in Scheme 1. The dendronized benzyl alcohol derivatives (**1** and **7**) were synthesized under Williamson etherification conditions from reaction of 3,5-dihydroxybenzyl alcohol and the corresponding bromides in 80 and 82% yields, respectively. Appel bromination of **1** and **7**, by reacting with CBr_4/PPh_3 in anhydrous dichloromethane or PBr_3 in anhydrous THF, can easily afford the dendronized benzyl bromides (**2** and **8**) with high yields of 90 and 80%, respectively. The dendritic monomer **1** and monomer **2** were prepared upon selective nucleophilic substitution reactions (SN) of the 9,9′-position of 2,7-dibromofluorene with corresponding bromide derivative in the presence of a strong alkali of NaOH in the DMSO solution.[17] The polymerization reaction was carried out via the well-known palladium-catalyzed Suzuki coupling reaction between 9,9-dihexylfluorene-2,7-bis(trimethylene boronate) and monomers **1** and **2** in THF to yield the pale-white solid of the corresponding copolymers (yield > 75%). The chemical structures of the copolymers were confirmed by ^{1}H NMR spectroscopy and elemental analysis, which all supported the formation of the resulting alternating copolymers. The molar feed ratios of monomer **1** to monomer **2** were 80:20, 50:50, and 20:80, and the corresponding copolymers were referred to as PFCO1, PFCO2, and PFCO3, respectively. The carbon contents for each copolymer, obtained from elemental analysis, were used for the calculation of actual copolymer composition. Thus, the values of x/y were determined to be 76:24, 42:58, and 17:83 for PFCO1, PFCO2, and PFCO3, respectively.

All the copolymers also have good solubility in common organic solvents, such as THF, CH_2Cl_2, $CHCl_3$ and toluene, etc., resulting from the hexyl side chains attached to the fluorene moiety and alkoxyl side chains linked to the phenyl units. Smooth and optically transparent thin solid films on ITO substrates were obtained by spin-coating the toluene solutions of these copolymers (10 mg mL^{-1}) at a spin rate of 1500 rpm. The molecular weights of the resulting copolymers were measured by gel permeation chromatography (GPC) with reference to polystyrene standards. As listed in Table 1, the copolymers have high weight-average molecular weights (M_n) of 16 800−19 600, with polydispersity indices (M_w/M_n) of 1.82−2.03. The thermal properties of the copolymers were determined from TGA and DSC measurements. All the copolymers exhibit good thermal stability, with onset decomposition temperatures (T_d) in the range of 393−409 °C

Table 2. Absorption and Emission Data for the Copolymers

	solution λ_{max}(nm)		film λ_{max}(nm)		Φ_{PL}		
copolymers	abs	em	abs	em	solution	film	optical band gap[a] (eV)
PFCO1	302, 387	418, 442	301, 387	426, 450	0.66	0.46	2.94
PFCO2	299, 389	418, 443	299, 389	425, 449	0.61	0.42	2.95
PFCO3	299, 386	419, 443	298, 386	424, 449	0.58	0.40	2.96

[a]Optical bandgap was estimated from the wavelength of the optical absorption edge of the polymer film.

under a nitrogen atmosphere. After the temperature was increased to above 400 °C, the weight loss increases abruptly, indicating the decomposition of the polymer backbones. Above 600 °C, there are only 27−40 wt % residues remaining, which were produced by charring during heating. The glass transition temperatures (T_g) of the copolymers range from 86 to 101 °C, which are higher than those of poly(9,9-dihexylfluorene) (PHF) (~55 °C).[18] Thus, the incorporation of a carbazole and oxadiazole functional dendronized units into the main chain has successfully increased the T_g of the polyfluorenes. The improved T_g is very important for these copolymers to be used as emissive materials in electroluminescence displays.[19]

Optical Properties. The optical properties of the copolymers were investigated both in solution and in the solid state. The concentration of the THF solutions of the copolymers was fixed at 1×10^{-6} M. PFCO1, PFCO2, and PFCO3 have similar UV−vis absorption spectra in THF solution (Figure 1). The respective shorter absorption maxima (λ_{max}) at about 302, 299, and 299 nm are due to the absorption of the carbazole and oxadiazole peripheral groups, which increase with the content of oxadiazole pendent units. The additional absorption peaks of PFCO1, PFCO2, and PFCO3 at 387, 389, and 386 nm are attributed to the $\pi-\pi^*$ transition associated with the conjugated polymer backbone. The absorption of these copolymers in solid films are similar to those in THF solutions. The absorption maxima are barely shifted in the solid thin films is observed, which indicates that large side dendrons can efficiently suppress the chain aggregation of fluorene-based polymers. In addition, the absorption onset wavelengths of PFCO1, PFCO2, and PFCO3 films were determined to be 421, 420, and 419 nm, which gives rise to the corresponding optical band gap of 2.94, 2.95, and 2.96 eV, respectively. The main features of these spectra are summarized in Table 2 and Figure 1.

The PL emission spectra of the copolymers in THF solutions (under 380 nm excitation) are shown in Figure 2. The maxima with two peaks appear at 418, 442 nm, 418, 443 nm, and 419, 443 nm for PFCO1, PFCO2, and PFCO3, respectively. The corresponding PL quantum yields (Φ_f) of these polymers in THF were 0.66, 0.61, and 0.58, when measured relative to that of 9,10-diphenylanthrancene ($\Phi_f = 0.9$).[20] Uniform and colorless polymer films were prepared on quartz substrates by s pin-coating from toluene solution of the respective polymers (10 mg mL^{-1}) at a spinning rate of 1500 rpm. The thickness of films was about 80 nm. Figure 2 also shows the PL spectra of the copolymers in thin film form. The PL maxima appear at 426, 450 nm, 425, 449 nm, and 424, 449 nm, which are only slightly red-shifted from their values in solution, suggesting that there was little aggregation of the chromophores or polymer main chains in the solid state. The PL quantum yields of the PFCO1, PFCO2, and PFCO3 films were estimated to be 0.46, 0.42, and 0.40, respectively, by comparing its fluorescence intensity to that of the polydihexylfluorene (PDHF) thin film excited at 380 nm ($\Phi_f = 0.55$).[3d] The emission spectral data are also summarized in Table 2.

The effect of annealing temperature on the color and luminescence stability is an important parameter in the

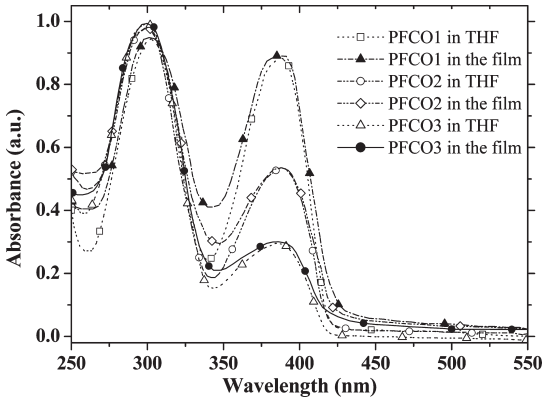

Figure 1. Absorption spectra of copolymers PFCO1, PFCO2, and PFCO3 in THF and solid-state films spin-coated on quartz plates.

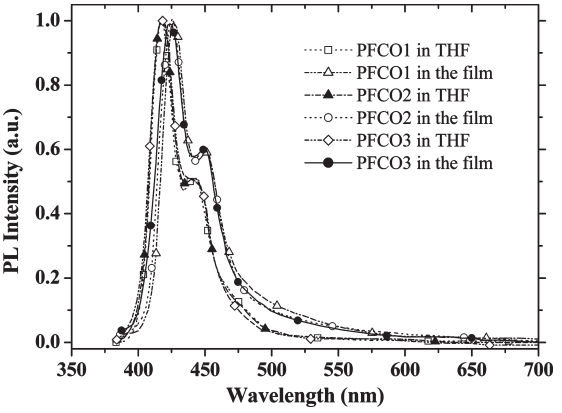

Figure 2. PL spectra of copolymers PFCO1, PFCO2, and PFCO3 in THF and solid-state films spin-coated on quartz plates.

performance of polymer light emitting devices (PLEDs). To examine the thermal stability of these copolymers, the spin-coated polymer films were treated at different temperatures and their PL spectra were systematically evaluated. A PDHF film was employed as the control. Figure 3 shows the normalized PL emission spectra of the resulting copolymers and PDHF films before and after thermal annealing. Thermal treatment of the PDHF film at 200 °C for 2 h led to an additional long wavelength emission at about 520 nm in the PL spectrum. The undesirable green emission that often develops in the PL and EL spectra of PFs has been attributed to physical (excimers or aggregates formation) and chemical (ketonic defects) degradation processes.[3c,3d] However, the resulting dendronized polymers exhibited good thermally stability, and their PL spectra did not show any significant red shifts after annealing at 200 °C for 2 h. Thus, with the introduction of dendronized side chains of functional carbazole and oxadiazole units into polyfluorenes, the red-shift phenomenon of PFs has been reduced markedly. Aggregation and excimer formation of the polymer chains have been avoided, resulting in improved stability and purity of the emission color.

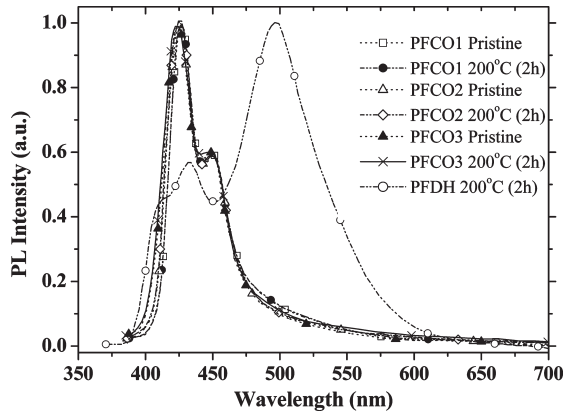

Figure 3. PL spectra (λ_{ex} = 380 nm) of the copolymer PFCO1, PFCO2, PFCO3, and PFDH films before and after thermal annealing at 200 °C for 2 h in air (PFDH = polydihexylfluorene).

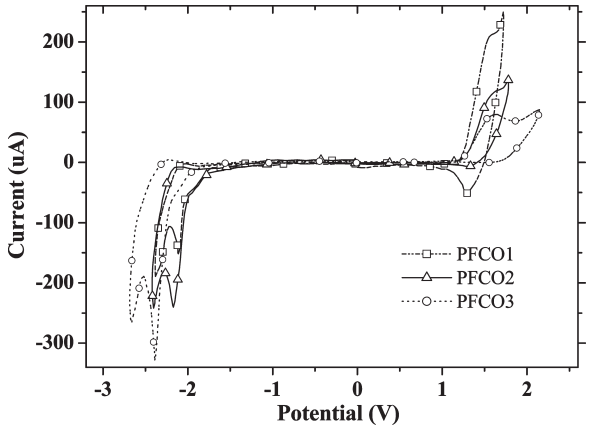

Figure 4. Cyclic voltammograms of the copolymer thin films coated onto platinum electrodes in an acetonitrile electrolyte solution of n-Bu_4NClO_4 (0.10 M), with a Ag/AgCl (0.10 M) reference electrode at room temperature (scan rate: 50 mV s^{-1}).

Electrochemical Properties. The redox behavior of the copolymer films on Pt plate electrodes was studied by cyclic voltammetry (CV), using a three-electrode cell in an anhydrous CH_3CN solution of 0.1 M tetrabutylammonium perchlorate (n-Bu_4NClO_4). A Pt wire was used as the counter electrode and Ag/AgCl (0.1 M) as the reference electrode. The energy level of the Ag/AgCl reference electrode (calibrated against the FC/FC^+ redox system) was 4.49 eV below the vacuum level. The cell was purged with pure argon prior to each scan. The scans toward the anodic and cathodic directions were performed separately at a scan rate of 50 mV s^{-1} at room temperature. As shown in Figure 4, all the copolymers show good reversibility in the n-doping and p-doping processes. On anodic sweep, the oxidation peak positions for PFCO1, PFCO2, and PFCO3 are at 1.59, 1.72 V, 1.65, 1.78 V, and 1.63, 2.14 V, respectively, with the corresponding rereduction peaks at 1.27, 1.33, and 1.56 V. The corresponding onset potentials of the p-doping process are determined to be 1.20, 1.19, and 1.16 V. Obviously, the increase in oxidation potentials of these copolymers compared to polyfluorene can be attributed to the high electron affinity of the oxadizazole groups incorporated into the polyfluorene main chains. On sweeping the polymers cathodically, the onset potentials of the n-doping process for PFCO1, PFCO2, and PFCO3 occur at about −1.74, −1.76, and −1.80 V, respectively, with the corresponding reduction potentials at −2.11, −2.37 V, −2.17, −2.41 V, and −2.39, −2.67 V and reoxidation peaks appearing at −2.03, −2.11, and −2.23 V. From the onset potentials of the oxidation and reduction processes, the bandgaps (E_g) of the PFCO1, PFCO2, and PFCO3 copolymers were estimated to be about 2.94, 2.95, and 2.96 eV, respectively. The value is quite close to those obtained by the optical method described above. The lowest unoccupied molecular orbital (LUMO) and highest occupied molecular orbital (HOMO) energy levels of the corresponding PFCO1, PFCO2, and PFCO3 copolymers are estimated to be −2.75, −2.73, and −2.69 eV and −5.69, −5.68, and −5.65 eV, respectively. The electrochemical data of the copolymers are summarized in Table 3. It is obvious that the bipolar nature of the carbazole and oxadiazole system can help to raise the HOMO energy level and reduce the LUMO level of the emitting materials. Therefore, the good electronic properties afforded by dendronized functional carbazole and oxadiazole side chains can give rise to efficient injection and transport of holes and electrons.

Table 3. Electrochemical Potentials and Energy Levels of the Copolymers

copolymers	$[E^{red}_{onset}]^a$ (V)	$[E^{ox}_{onset}]^b$ (V)	LUMO^c (eV)	HOMO^d (eV)	$E_g{}^e$ (eV)
PFCO1	1.20	−1.74	−2.75	−5.69	2.94
PFCO2	1.19	−1.76	−2.73	−5.68	2.95
PFCO3	1.16	−1.80	−2.69	−5.65	2.96

[a]Onset reduction potentials measured by cyclic voltammetry. [b]Onset oxidation potential measured by cyclic voltammetry. [c]Calculated from the reduction potentials. [d]Calculated from the oxidation potentials. [e]Calculated from the LUMO and HOMO energy levels.

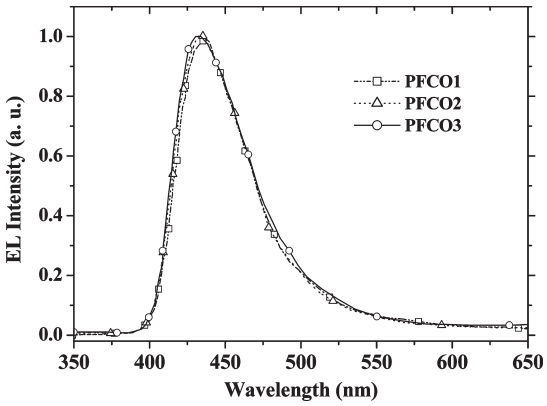

Figure 5. EL spectra of devices based on PFCO1, PFCO2, and PFCO3 copolymers with the configuration of ITO/PEDOT/copolymer/TPBI/LiF/Al.

EL Properties of the PLED Devices. Standard PLED devices with the configuration of ITO/PEDOT (60 nm)/copolymer (80 nm)/TPBI (20 nm)/LiF (1 nm)/Al (150 nm) were fabricated and evaluated. 1,3,5-Tris(N-phenylbenzimidazol-2-yl)benzene (TPBI) was used as the hole-blocking layer and the electrontransporting layer. The EL spectra of these dendronized copolymers are similar to the PL spectra of the corresponding copolymer films, which indicated that the emission from these devices originated from the dendronized copolymers. However, the shape of the EL spectra made little difference because there is only one peak in the EL spectra compared with their PL spectra. This is caused by the different excitation processes involved for PL and EL. In other words, the electron states of these materials have the little difference between photoexcitation and electroexcitation.[6f] As shown in Figure 5, the maxima in the EL spectra occurred at about 437, 434, and 432 nm for the devices based on PFCO1, PFCO2, and PFCO3, respectively. The green emission from the PFs were not observed in all of these devices. The larger shielding effect of dendronized carbazole

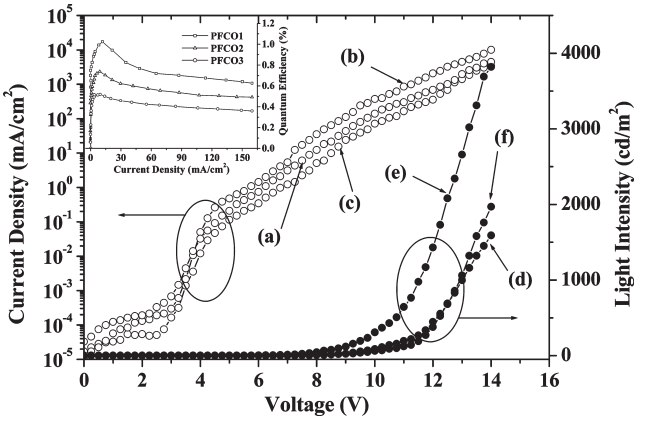

Figure 6. Current density−voltage ($J-V$) and light intensity−voltage ($L-V$) curves for the ITO/PEDOT/copolymer/TPBI/LiF/Al device configuration. Curves (a) and (d) were recorded from the device based on PFCO1, (b) and (e) from the device based on PFCO2, and (c) and (f) from the device based on PFCO3. Inset: quantum efficiency−current density curves of the devices based on copolymer PFCO1, PFCO2, and PFCO3.

and oxadiazole side chains has efficiently suppressed the aggregates/excimers of polymer main chains to give rise to the more pure blue emission. Obviously, increase of the content of dendronized functional oxadiazole units will make the maximum peak of EL spectrum blue shift. Current density−voltage ($J-V$) and light intensity−voltage ($L-V$) characteristics of the PLED devices indicated that the current density and luminance increased exponentially with the increase in forward bias voltage. The behavior was characteristic of that of a diode. The turn-on voltages of these PLEDs based on PFCO1, PFCO2, and PFCO3 were 6.8, 5.5, and 6.5 V, respectively. The maximum EL efficiencies of the devices based on PFCO1, PFCO2, and PFCO3 were measured to be 1.03% (with a current density of 12 mA cm^{-2}), 0.74% (with a current density of 9 mA cm^{-2}), and 0.52% (with a current density of 10 mA cm^{-2}), respectively. From the performance values, the device based on PFCO1 is the best, which indicated the copolymer has the closest match of the carrier injection and transport in this case. After increasing the content of dendronized functional oxadiazole units, the device performance became worse. The reason can be attributed to the larger influence on the trapping process by dendronized oxadiazole side chains than carbazole. These results are described in Figure 6.

Owing to the excellent overlap of the emission bands of these copolymers with the excitation bands of most phosphorescent emitting materials (around 400−450 nm), they are expected to be excellent host materials for phosphorescent emitting diodes. To investigate the versatility of these dendronized copolymers as host materials, triple-layer EL devices with a configuration of ITO/PEDOT (60 nm)/copolymer:$(tpbi)_2Ir(acac)$ (80 nm)/Ca (4 nm)/Al (150 nm) were fabricated. The emissive layer consists of the host materials of PFCO1, PFCO2, or PFCO3 doped with 4 wt % $(tpbi)_2Ir(acac)$. All the devices emitted bright green light, and there no blue emission was observed, implying the completely efficient energy transfer from the host copolymers to the phosphorescent emitters. The typical EL spectra are shown in Figure 7. Compared with our previous work, the emissions originate from the phosphorescent emitter of $(tpbi)_2Ir(acac)$.[21] Figure 8 shows the current density−voltage ($J-V$) and light intensity−voltage ($L-V$) characteristics of these phosphorescent PLED devices. The maximum EL efficiencies of the devices based on PFCO1, PFCO2, and PFCO3 were measured to be 11.63%, 7.90%, and 5.23%, respectively.

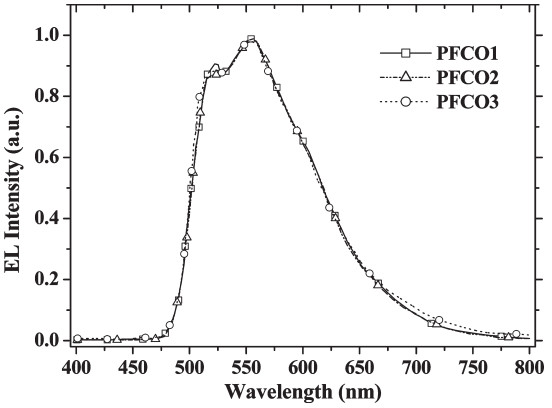

Figure 7. EL spectra of devices used PFCO1, PFCO2, and PFCO3 copolymers as host materials with the configuration of ITO/PEDOT/copolymer:$(tpbi)_2Ir(acac)$/Ca/Al.

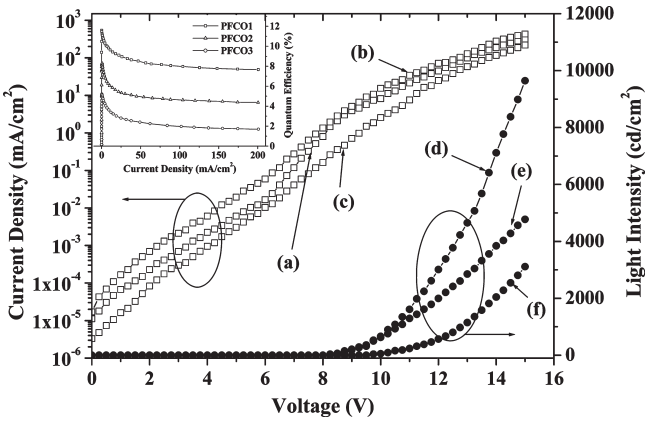

Figure 8. Current density−voltage ($J-V$) and light intensity−voltage ($L-V$) curves for the ITO/PEDOT/copolymer:$(tpbi)_2Ir(acac)$/Ca/Al device configuration. Curves (a) and (d) were recorded from the device based on PFCO1, (b) and (e) from the device based on PFCO2, and (c) and (f) from the device based on PFCO3. Inset: quantum efficiency−current density curves of the devices based on copolymer PFCO1, PFCO2, and PFCO3.

All these devices have more sample configuration and more better performance without inserting the PVK hole transport layer and mixing the PBD electron transport materials, which indicated that these copolymers with dendronized functional cabazole and oxadiazole side chains are better candicates of host materials for $(tpbi)_2Ir(acac)$ emitter than poly(9,9-di-*n*-octylfluorene-2,7-diyl) (PFO).[21] The best performance was obtained for the device based on PFCO1 doped with $(tpbi)_2Ir(acac)$. The results show that the copolymer with 80% content of dendronized cabazole side chains possesses the optimized composition as the host materials. Increasing the content of dendronized oxazole side chains more than 20%, the performance of devices decreases gradually from PFCO2 to PFCO3. From above, attaching the dendronized functional cabazole and oxazole side chains to the backbone of polyfluorenes can not only decrease the aggregates of the polymer main chains to afford better blue color purity but also balance the carriers injection and transport for phosphorescent and non-phosphorescent PLEDs.

Conclusions

A series of new polyfluorenes with dendronized functional cabazole and oxazole side chains have been successfully synthesized and characterized. These copolymers show good thermal properties and solubility in organic solvents. The PL and EL

emission color quality was improved very much due to less aggregates of main chains of polyfluorenes with the steric hindrance of dendronized functional units. The electroluminescent devices based on these copolymers as blue emitters and host materilas show balanced carriers injection and transport in both nonphosphorescent and phosphorescent PLEDs. The best devices were obstained by using PFCO1 materilas with the exteral quantum efficiencies of 1.03 and 11.63%, respectively. The results indicated that these copolymers were promising candicates to be used as both efficient pure blue emitters and host materials for highly efficient phosphorescent PLEDs.

Experimental Section

Instruments. ^{1}HNMR spectra were recorded on a Bruker ACF 400 spectrometer with *d*-chloroform as the solvent and tetramethylsilane as the internal standard. Number-average (M_n) and weight-average (M_w) molecular weights were determined on a HP 1100 HPLC system equipped with a HP 1047A RI detector and Agilent PLgel MIXED-C300 × 7.5 mm (ID) columns (packed with 5 μm particles of different pore sizes). THF was used as the eluent at a flow rate of 10 mL min^{-1} at 35 °C. Polystyrene standards were used as the molecular weight references. Cyclic voltammetry measurements were made on an AUTOLAB potentiostat/galvanostat electrochemical workstation at a scan rate of 50 mV/s, with a platinum wire counter electrode and an Ag/AgCl reference electrode in an anhydrous and nitrogen-saturated 0.1 mol/L acetonitrile (CH_3CN) solution of tetrabutylammonium perchlorate (Bu_4NClO_4). The copolymers were coated on the platinum plate working electrodes from dilute chloroform solutions. UV−vis and fluorescence spectra were obtained on a Carry 300 spectrophotometer and a Carry Eclipse photoluminescence spectrophotometer, respectively. Thermogravimetric analyses (TGA) were conducted on a TA Instruments TGA 2050 thermogravimetric analyzer at a heating rate of 10 °C min^{-1} and under an N_2 flow rate of 90 mL min^{-1}. Differential scanning calorimetry (DSC) measurements were carried out on a Mettler Toledo DSC 822e system under N_2 and at a heating rate of 10 °C min^{-1}.

Materials. 9-(6-Bromohexyl)-9*H*-carbazole, 3,5-bis[4-(9*H*-carbazol-9-yl)hexyloxy]benzyl alcohol (**1**), 3,5-bis[4-(9*H*-carbazol-9-yl)hexyloxy]benzyl bromide (**2**), and 9,9-dihexylfluorene-2,7-bis(trimethylene boronates) were synthesized according to the literature procedures.[9b,22] The solvents were dried using standard procedures and purged with nitrogen. All other reagents were used as received from commercial sources without further treatments.

Preparation of Monomers. *Monomer **1***. A mixture of 2,7-dibromofluorene (0.154 g, 0.48 mmol) and tetrabutylammonium chloride (2.78 mg, 0.01 mmol) in 60 mL of DMSO was degassed for 10 min, and then 2 mL of aqueous NaOH solution (50%) was added and stirred vigorously for 10 min under nitrogen. To this mixture was added the solution of **2** (0.718 g, 1 mmol) in 80 mL of degassed DMSO under nitrogen. The mixture was stirred under nitrogen for 8 h, water was added, and the aqueous layer was extracted with CH_2Cl_2 (50 mL × 3). The combined organic phases were dried over $MgSO_4$. After removal the solvent, the residue was purified by column chromatography with CH_2Cl_2/petroleum ether (4:1, v/v) to give pale-yellow solid with a yield of 80%. ^{1}H NMR ($CDCl_3$, 400 MHz, δ/ppm): 8.12 (d, 8H), 7.53 (s, 2H), 7.45 (t, 8H), 7.35 (t, 8H), 7.22 (t, 8H), 7.10 (d, 2H), 6.96 (d, 2H), 6.10 (s, 2H), 5.81 (s, 4H), 4.34 (t, 8H), 3.68 (t, 8H), 3.18 (s, 4H), 1.96−1.72 (m, 32H). Anal. Calcd for $C_{99}H_{96}N_4O_4Br_2$: C, 75.95%; H, 6.18%; N, 3.58%. Found: C, 75.69%; H, 6.06%; N, 3.64%.

*4-Methylbenzoic Acid N′-[4-hexyloxybenzoyl] Hydrazide (**4**)*. To a mixture of 4-(hexyloxy)benzoic acid hydrazide (5.91 g, 25 mmol), 1 mL of pyridine, and 15 mL of tetrahydrofuran, 4-methylbenzoyl chloride (4.72 g, 30.5 mmol) was added quickly under nitrogen. The reaction mixture was stirred at 60 °C for 12 h and then poured into water. The precipitate was filtered and recrystallized from methanol to afford a white solid with a yield of 85%. ^{1}H NMR ($CDCl_3$, 400 MHz, δ/ppm): 9.82 (d, 1H), 9.51 (d, 1H), 7.45 (t, 8H), 7.86 (d, 2H), 7.80 (d, 2H), 7.42 (d, 2H), 6.96 (d, 2H), 6.90 (d, 2H), 4.62 (s, 2H), 4.01 (d, 2H), 2.32 (t, 3H), 1.62−0.86 (m, 11H). Anal. Calcd for $C_{21}H_{26}N_2O_3$: C, 71.16%; H, 7.39%; N, 7.90%. Found: C, 71.12%; H, 7.36%; N, 7.96%.

*2-(4-Methylphenyl)-5-[4-hexyloxyphenyl]-[1,3,4]oxadiazole (**5**)*. A mixture of **4** (1.77 g, 5 mmol) in 10 mL of $SOCl_2$ was refluxed for 6 h under a nitrogen atmosphere. Excess $SOCl_2$ was distilled off, and then the residue was slowly poured into 50 mL of water to give a precipitate. The crude produce was purified by column chromatography with CH_2Cl_2 to yield white solid with a yield of 72%. ^{1}H NMR ($CDCl_3$, 400 MHz, δ/ppm): 8.10 (d, 2H), 8.02 (d, 2H), 7.36 (d, 2H), 6.88 (d, 2H), 3.90 (d, 2H), 2.42 (s, 3H), 1.67−0.88 (m, 11H). Anal. Calcd for $C_{21}H_{24}N_2O_2$: C, 74.97%; H, 7.19%; N, 8.33%. Found: C, 74.94%; H, 7.16%; N, 8.38%.

*2-(4-Bromomethylphenyl)-5-[4-hexyloxyphenyl]-[1,3,4]oxadiazole (**6**)*. To a solution of **5** (5.75 g, 17.1 mmol) and dibenzoyl peroxide (catalytic amount) in 20 mL of CCl_4 was added *n*-bromosuccinimide (NBS) (6.10 g, 34.3 mmol). The reactant mixture was refluxed for 5 h under a nitrogen atmosphere. The solvent was distilled off, and then the residue was purified by column chromatography with CH_2Cl_2 to yield white solid with a yield of 65%. ^{1}H NMR ($CDCl_3$, 400 MHz, δ/ppm): 8.16 (d, 2H), 8.05 (d, 2H), 7.56 (d, 2H), 7.02 (d, 2H), 4.63 (s, 2H), 3.93 (d, 2H), 1.68−0.89 (m, 11H). Anal. Calcd for $C_{21}H_{23}N_2O_2Br$: C, 60.73%; H, 5.58%; N, 6.75%. Found: C,60.70%; H, 5.53%; N, 6.79%.

*(3,5-Bis{4-[5-(4-hexyloxyphenyl)-[1,3,4]oxadiazol-2-yl]benzyloxy}phenyl)methanol (**7**)*. A mixture of **6** (6.48 g, 15.6 mmol), 3,5-dihydroxybenzyl alcohol (1.00 g, 7.1 mmol), potassium carbonate (3.68 g, 65 mmol), and 18-crown-6 (0.38 g, 1.42 mmol) in 60 mL of anhydrous acetone was refluxed with vigorous stirring under nitrogen for 60 h. The mixture was cooled to room temperature, and the solvent was evaporated under reduced pressure. The residue was extracted between CH_2Cl_2 and deionized water. Afterward, the aqueous layer was extracted with CH_2Cl_2 (50 mL × 3). The combined extracts were dried with anhydrous $MgSO_4$ and evaporated. The crude product was purified by column chromatography on silica gel eluting with CH_2Cl_2 to give **7** as a pale yellow solid with a yield of 82%. ^{1}H NMR ($CDCl_3$, 400 MHz, δ/ppm): 8.16 (d, 4H), 8.06 (d, 4H), 7.56 (d, 4H), 7.28 (s, 1H), 7.05 (d, 4H), 6.72 (s, 2H), 6.50 (s, 1H), 5.21 (s, 4H), 4.70 (s, 2H), 3.90 (t, 4H), 1.89−1.78 (m, 22H). Anal. Calcd for $C_{49}H_{52}N_4O_7$: C, 72.75%; H, 6.48%; N, 6.93%. Found: C, 72.70%; H, 6.45%; N, 6.98%.

*(3,5-Bis{4-[5-(4-hexyloxyphenyl)-[1,3,4]oxadiazol-2-yl]benzyloxy}phenyl)benzyl Bromide (**8**)*. To a mixture of **7** (0.81 g, 1 mmol) and 15 mL of THF was added dropwise the solution of PBr_3 (0.27 g, 1 mmol) in 5 mL of THF over 15 min at 0 °C. The reactant mixture was heated to reflux for 30 min. After the solution was cooled to room temperature, the solvent was evaporated off. The residue was purified by column chromatography with ethyl acetate/CH_2Cl_2 (v:v = 1:10) to afford a white solid with a yield of 80%. ^{1}H NMR ($CDCl_3$, 400 MHz, δ/ppm): 8.15 (d, 4H), 8.05 (d, 4H), 7.57 (d, 4H), 7.04 (d, 4H), 6.70 (s, 2H), 6.54 (s, 1H), 5.16 (s, 4H), 4.48 (s, 2H), 3.92 (t, 4H), 1.89−1.78 (m, 22H). Anal. Calcd for $C_{49}H_{51}N_4O_6Br$: C, 67.51%; H, 5.90%; N, 6.43%. Found: C, 67.47%; H, 5.88%; N, 6.54%.

*Monomer **2***. A mixture of 2,7-dibromofluorene (0.154 g, 0.48 mmol) and tetrabutylammonium chloride (2.78 mg, 0.01 mmol) in 60 mL of DMSO was degassed for 10 min, and then 2 mL of aqueous NaOH solution (50%) was added and stirred vigorously for 10 min under nitrogen. To this mixture was added the solution of **8** (0.872 g, 1 mmol) in 80 mL of degassed DMSO under nitrogen. The mixture was stirred under nitrogen for 10 h, water was added, and the aqueous layer was extracted with CH_2Cl_2 (50 mL × 3). The combined organic phases were dried over $MgSO_4$. After removal the solution, the residue was purified by column chromatography with ethyl acetate/CH_2Cl_2 (v:v = 1:1) to give pale-yellow solid with a yield of 62%. ^{1}H NMR ($CDCl_3$, 400 MHz, δ/ppm): 8.11 (d, 8H),

8.06 (d, 8H), 7.56 (s, 2H), 7.46 (t, 8H), 7.40 (d, 2H), 7.23 (d, 2H), 7.08 (d, 8H), 6.34 (s, 2H), 5.92 (s, 4H), 4.82 (s, 8H), 4.30 (t, 8H), 3.18 (s, 4H), 1.92- 1.73 (m, 44H). Anal. Calcd for $C_{115}H_{108}N_8O_{12}Br_2$: C, 70.69%; H, 5.57%; N, 5.73%. Found: C, 70.63%; H, 5.53%; N, 5.78%.

General Synthetic Procedure for Dendronized Copolymers. To a mixture of 9,9-dihexylfluorene-2,7-bis(trimethylene boronates), monomer **1**, monomer **2**, $Pd(PPh_3)_4$, and three drops of Aliquat 336 was added a mixture of THF and aqueous 2 M potassium carbonate. The mixture was vigorously stirred at 90 °C for 72 h. After the mixture was cooled to room temperature, it was poured into 500 mL of methanol and deionized water (10:1). A fibrous solid was obtained by filtration, and the solid was washed with methanol, water, and methanol again. After washing for 24 h in a Soxhlet apparatus with acetone, the resulting dendronized copolymer was obtained as a pale solid after drying under vacuum.

PFCO1. 9,9-Dihexylfluorene-2,7-bis(trimethylene boronates) (279.5 mg, 0.56 mmol), monomer **1** (665.6 mg, 0.448 mmol), monomer **2** (218.8 mg, 0.112 mmol), $Pd(PPh_3)_4$ (12 mg), Aliquat 336 (three drops), THF (25 mL), and aqueous 2 M potassium carbonate (6 mL) were used in the reaction mixture. Yield: 82%. ^{1}H NMR ($CDCl_3$, 400 MHz, δ/ppm): 8.06−8.00 (m, 9H), 7.85−7.63 (m, 18H), 7.42−7.11 (m, 26H), 6.92 (d, 2H), 6.34 (s, 5H), 6.08 (s, 2.5H), 4.80−4.72 (t, 2H), 4.24−4.16 (t, 8H), 3.92−3.86 (d, 10H), 3.43 (br, 5H), 2.04 (br, 5H), 1.82−0.71 (m, 70.5H). Anal. Calcd for $(C_{158}H_{163}N_6O_7)_n$: C, 84.04%; H, 7.28%; N, 3.72%. Found: C, 83.73%; H, 7.12%; N, 3.89%.

PFCO2. 9,9-Dihexylfluorene-2,7-bis(trimethylene boronates) (279.5 mg, 0.56 mmol), monomer **1** (416.0 mg, 0.28 mmol), monomer **2** (547.1 mg, 0.28 mmol), $Pd(PPh_3)_4$ (12 mg), Aliquat 336 (three drops), THF (25 mL), and aqueous 2 M potassium carbonate (6 mL) were used in the reaction mixture. Yield: 80%. ^{1}H NMR ($CDCl_3$, 400 MHz, δ/ppm): 8.08−8.01 (m, 24H), 7.86−7.62 (m, 24H), 7.44−7.12 (m, 32H), 6.93 (d, 8H), 6.34 (s, 8H), 6.09 (s, 4H), 4.82−4.73 (t, 8H), 4.26−4.16 (t, 8H), 3.94−3.88 (d, 16H), 3.42 (br, 8H), 2.06 (br, 8H), 1.83−0.72 (m, 120H). Anal. Calcd for $(C_{260}H_{268}N_{12}O_{16})_n$: C, 81.81%; H, 7.08%; N, 4.40%. Found: C, 81.20%; H, 6.98%; N, 4.56%.

PFCO3. 9,9-Dihexylfluorene-2,7-bis(trimethylene boronates) (279.5 mg, 0.56 mmol), monomer **1** (166.4 mg, 0.112 mmol), monomer **2** (875.4 mg, 0.448 mmol), $Pd(PPh_3)_4$ (12 mg), Aliquat 336 (three drops), THF (25 mL), and aqueous 2 M potassium carbonate (6 mL) were used in the reaction mixture. Yield: 77%. ^{1}H NMR ($CDCl_3$, 400 MHz, δ/ppm): 8.10−8.02 (m, 21H), 7.88−7.61 (m, 12H), 7.45−7.11 (m, 14H), 6.92 (d, 8H), 6.34 (s, 5H), 6.10 (s, 2.5H), 4.80−4.71 (t, 8H), 4.24−4.14 (t, 2H), 3.98−3.90 (d, 10H), 3.43 (br, 5H), 2.05 (br, 5H), 1.85−0.74 (m, 79.5H). Anal. Calcd for $(C_{167}H_{172}N_9O_{13})_n$: C, 79.81%; H, 6.90%; N, 5.02%. Found: C, 79.62%; H, 6.82%; N, 5.13%.

Acknowledgment. This work was supported by the Natural Science Foundation of China (NSFC, Grant 20802033), Scientific Research Foundation for Returned Scholars, Ministry of Education of China, Natural Science Foundation of Jiangxi Province (Grant 2007GZC1552), Scientific Research Project of Educational Commission of Jiangxi Province (Grant GJJ09178), and Scientific Research Foundation of Nanchang Hangkong University (Grant EA200802012).

References and Notes

(1) (a) Burroughes, J. H.; Bradley, D. D. C.; Brown, A. B.; Marks, R. N.; Mackay, K.; Friend, R. H.; Burn, P. L.; Holmes, A. B. *Nature (London)* **1990**, *347*, 539. (b) Hide, F.; Diaz-Garcia, M. A.; Schwartz, B. J.; Heeger, A. J. *Acc. Chem. Res.* **1997**, *30*, 430. (c) Friend, R. H.; Gymer, R. W.; Holmes, A. B.; Burroughes, J. H.; Marks, R. N.; Taliani, C.; Bradley, D. D. C.; Dos Santos, D. A.; Brédas, J. L.; Lögdlund, M.; Salaneck, W. R. *Nature (London)* **1999**, *397*, 121. (d) Müller, D. C.; Falcou, A.; Reckefuss, N.; Rojahn, M.; Wlederhirm, V.; Rudati, P.; Frohne, H.; Nuyken, O.; Becker, H.; Meerhotz, K. *Nature (London)* **2003**, *421*, 829.

(2) (a) Woudenbergh, T. V.; Wildeman, J.; Blom, P. W. M.; Bastiaansen, J. J. A. M.; Langeveld-Voss, B. M. W. *Adv. Funct. Mater.* **2004**, *14*, 677. (b) Culligan, S. W.; Geng, Y.; Chen, S. H.; Klubek, K.; Vaeth, K. M.; Tang, C. W. *Adv. Mater.* **2003**, *15*, 1176. (c) Yan, H.; Huang, Q.; Cui, J.; Veinot, J. G. C.; Kern, M. M.; Marks, T. J. *Adv. Mater.* **2003**, *15*, 835. (d) Suh, M. C.; Chin, B. D.; Kim, M.; Kang, T. M.; Lee, S. T. *Adv. Mater.* **2003**, *15*, 1254. (e) Lo, S.; Fichards, G. J.; Markham, J. P. J.; Namdas, E. B.; Sharma, S.; Burn, P. L.; Samuel, I. D. W. *Adv. Funct. Mater.* **2005**, *15*, 1451. (f) Lu, H.; Liu, C.; Chang, C.; Chen, S. *Adv. Mater.* **2007**, *19*, 2574. (g) Liu, J.; Zou, J. H.; Yang, W.; Wu, H. B.; Li, C.; Zhang, B.; Peng, J. B.; Cao, Y. *Chem. Mater.* **2008**, *20*, 4499.

(3) (a) Bernius, M. T.; Inbasekaran, M.; O'Brien, J.; Wu, W. W. *Adv. Mater.* **2000**, *12*, 1737. (b) Kreyenschmidt, M.; Klaerner, G.; Fuhrer, T.; Ashenhurst, J.; Karg, S.; Chen, W. D.; Lee, V. Y.; Scoot, J. C.; Miller, R. D. *Macromolecules* **1998**, *31*, 1099. (c) Neher, D. *Macromol. Rapid Commun.* **2001**, *22*, 1365. (d) Scherf, U.; List, E. J. W. *Adv. Mater.* **2002**, *14*, 477. (e) Peng, Q.; Xie, M. G.; Huang, Y.; Lu, Z. Y.; Xiao, D. *J. Polym. Sci., Part A: Polym. Chem.* **2004**, *42*, 2985.

(4) (a) Teetsov, J.; Fox, M. A. *J. Mater. Chem.* **1999**, *9*, 2117. (b) List, E. J. W.; Guentner, R.; De Freitas, P. S.; Scherf, U. *Adv. Mater.* **2002**, *14*, 374. (c) Romaner, L.; Pogantsch, A.; De Freitas, P. S.; Scherf, U.; Gaal, M.; Zojer, E.; List, E. J. W. *Adv. Funct. Mater.* **2003**, *13*, 597. (d) Peng, Q.; Peng, J. B.; Kang, E. T.; Neoh, K. G.; Cao, Y. *Macromolecules* **2005**, *38*, 7292.

(5) Gaal, M.; List, E. J. W.; Scherf, U. *Macromolecules* **2003**, *36*, 4236.

(6) (a) Lim, E.; Jung, B. J.; Shim, H. K. *Macromolecules* **2003**, *36*, 4288. (b) Marsitzky, D.; Vestberg, R.; Blainey, P.; Tang, B. T.; Hawker, C. J.; Carter, K. R. *J. Am. Chem. Soc.* **2001**, *123*, 6965. (c) Setayesh, S.; Grimsdale, A. C.; Weil, T.; Enkelmann, V.; Müllen, K.; Meghdadi, F.; List, E. J. W.; Leising, G. *J. Am. Chem. Soc.* **2001**, *123*, 946. (d) Pogantsch, A.; Wenzl, F. P.; List, E. J. W.; Leising, G.; Grimsdale, A. C.; Müllen, K. *Adv. Mater.* **2002**, *14*, 1061. (e) Shu, C. F.; Dodda, R.; Wu, I. F.; Liu, M. S.; Jen, A. K. Y. *Macromolecules* **2003**, *36*, 6698. (f) Zeng, G.; Yu, W. L.; Chua, S. J.; Huang, W. *Macromolecules* **2002**, *35*, 6907. (f) Peng, Q.; Xie, M. G.; Huang, Y.; Lu, Z. Y.; Xiao, D. *J. Polym. Sci., Part A: Polym. Chem.* **2004**, *42*, 2985.

(7) (a) Setayesh, S.; Grimsdale, A. C.; Weil, T.; Enkelmann, V.; Müllen, K.; Meghdadi, F.; List, E. J. W.; Leising, G. *J. Am. Chem. Soc.* **2001**, *123*, 946. (b) Pogantsch, A.; Wenzl, F. P.; List, E. J. W.; Leising, G.; Grimscale, A. C.; Müllen, K. *Adv. Mater.* **2002**, *14*, 1061.

(8) (a) Marsitzky, D.; Vestberg, R.; Blainey, P.; Tang, B. T.; Hawker, C. J.; Carter, K. R. *J. Am. Chem. Soc.* **2001**, *123*, 6965. (b) Tang, H. Z.; Fujiki, M.; Zhang, Z. B.; Torimitsu, K.; Motonaga, M. *Chem. Commun.* **2001**, 2426. (c) Chou, C. H.; Shu, C. F. *Macromolecules* **2002**, *35*, 9673.

(9) (a) Fu, Y. Q.; Li, Y.; Li, J.; Yan, S.; Bo, Z. S. *Macromolecules* **2004**, *37*, 6395. (b) Peng, Q.; Li, M. J.; Lu, S. Q.; Tang, X. H. *Macromol. Rapid Commun.* **2007**, *28*, 785. (c) Wu, C. W.; Sung, H. H.; Lin, H. C. *J. Polym. Sci., Part A: Polym. Chem.* **2006**, *44*, 6765.

(10) (a) Koher, A.; Wilson, J. S.; Friend, R. H. *Adv. Eng. Mater.* **2002**, *4*, 453. (b) Holder, E.; Langeveld, B. M. W.; Schubert, U. S. *Adv. Mater.* **2005**, *17*, 1109. (c) Adachi, C.; Baldo, M. A.; Thompson, M. E.; Forrest, S. R. *J. Appl. Phys.* **2001**, *90*, 5048.

(11) (a) Lee, C. L.; Lee, K. B.; Kim, J. J. *Appl. Phys. Lett.* **2000**, *77*, 2280. (b) Vaeth, K. M.; Tang, C. W. *J. Appl. Phys.* **2002**, *92*, 3447. (c) Kawamura, Y.; Yanagida, S.; Forrest, S. R. *J. Appl. Phys.* **2002**, *92*, 87. (d) Gong, X.; Ostrowski, J. C.; Bazan, G. C.; Moses, D.; Heeger, A. J.; Liu, M. S.; Jen, A. K. Y. *Adv. Mater.* **2003**, *15*, 45.

(12) Cleave, V.; Yahioglu, G.; Le Barny, P.; Friend, R. H.; Tessler, N. *Adv. Mater.* **1999**, *11*, 285.

(13) Shoustikov, A. A.; You, Y.; Tompson, M. E. *IEEE J. Sel. Top. Quantum Electron.* **1998**, *4*, 3.

(14) (a) Liu, Q. D.; Lu, J. P.; Ding, J. F.; Day, M.; Tao, Y.; Barrios, P.; Stupak, J.; Chan, K.; Li, J. J.; Chen, Y. *Adv. Funct. Mater.* **2007**, *17*, 1028. (b) Yeh, K. M.; Lee, C. C.; Chen, Y. *J. Polym. Sci., Part A: Polym. Chem.* **2008**, *46*, 5180. (c) Yeh, K. M.; Lee, C. C.; Chen, Y. *Polymer* **2008**, *49*, 4211.

(15) (a) Tao, X. T.; Zhang, Y. D.; Wada, T.; Sasabe, H.; Suzuki, H.; Watanabe, T.; Miyata, S. *Adv. Mater.* **1998**, *10*, 226. (b) Kimoto, A.; Cho, J. S.; Higuchi, M.; Yamamoto, K. *Macromolecules* **2004**, *37*, 5531.

(16) (a) Kraft, A.; Grimsdale, A. C.; Holmes, A. B. *Angew. Chem., Int. Ed.* **1998**, *37*, 402. (b) Yu, W. L.; Meng, H.; Pei, J.; Huang, W. *J. Am. Chem. Soc.* **1998**, *120*, 11808. (c) Peng, Z.; Zhang, J. *Chem. Mater.* **1999**, *11*, 1138. (d) Mitschke, U.; Bäuerle, P. *J. Mater. Chem.* **2000**, *10*, 1471.

(17) Marsitzky, D.; Vestberg, R.; Blainey, P.; Tang, B. T.; Hawker, C. J.; Carter, K. R. *J. Am. Chem. Soc.* **2001**, *123*, 6965.

(18) Fukuda, M.; Sawada, K.; Yoshino, K. *J. Polym. Sci., Part A: Polym. Chem.* **1990**, *31*, 2465.
(19) Tokito, S.; Tanaka, H.; Noda, K.; Okada, A.; Taga, Y. *Appl. Phys. Lett*. **1997**, *70*, 1929.
(20) Eaton, D. *Pure Appl. Chem*. **1998**, *60*, 1107.
(21) Wei, X. Q.; Peng, J. B.; Cheng, J. B.; Xie, M. G.; Lu, Z. Y.; Li, C.; Cao, Y. *Adv. Funct. Mater*. **2007**, *17*, 3319.
(22) Yu, W. L.; Pei, J.; Cao, Y.; Huang, W.; Heeger, A. J. *Chem. Commun*. **1999**, 1837.